frontiers in Materials

ORIGINAL RESEARCH
published: 26 October 2021
doi: 10.3389/fmats.2021.765427

Inverted Hysteresis Loops in the $Fe_{73.5}Cu_1Nb_3Si_{13.5}B_9$ Alloy With Small Coercivity

P. P. Shen[1,2], *Y. T. Wang*[1,2] *and B. A. Sun*[1,2,3]*

[1]*Institute of Physics, Chinese Academy of Sciences, Beijing, China,* [2]*School of physical Science, University of Chinese Academy of Sciences, Beijing, China,* [3]*Songshan Lake Materials Laboratory, Dongguan, China*

The phenomenon of inverted hysteresis loop has been observed in many materials for the past decades. However, the physical origin of the inverted hysteresis loop has long been debated. Here, we report the completely inverted hysteresis loop with a clockwise cycle in the soft-magnetic nanocrystalline $Fe_{73.5}Cu_1Nb_3Si_{13.5}B_9$ alloy and amorphous $Fe_{73.5}Cu_1Nb_3Si_{13.5}B_9$ alloy at room temperature. The negative remanence and positive coercivity were observed in the descending branch of magnetization curve when the scan field range was above 1 KOe. By comparing the results with that of the standard Pd sample, we found that the net coercivities of the nanocrystalline $Fe_{73.5}Cu_1Nb_3Si_{13.5}B_9$ alloy and standard Pd sample are almost equal for the different scanning field ranges. Therefore, it is confirmed that the phenomenon of completely inverted hysteresis loop is caused by the remanence of superconducting magnet rather than the structural inhomogeneity effects. Our results suggest that special care should be taken during the measurement of hysteresis loops using MPMS 3, especially for the materials with small coercivity.

Keywords: hysteresis loop, amorphous alloys, soft magnetic alloy, coercivity, nanocrystalline

OPEN ACCESS

Edited by:
Jiang Ma,
Shenzhen University, China

Reviewed by:
Bo Huang,
Shanghai University, China
Fanli Meng,
Northeastern University, China

****Correspondence:***
B. A. Sun
sunba@iphy.ac.cn

Specialty section:
This article was submitted to Ceramics and Glass, a section of the journal Frontiers in Materials

Received: *27 August 2021*
Accepted: *23 September 2021*
Published: *26 October 2021*

Citation:
Shen PP, Wang YT and Sun BA (2021) Inverted Hysteresis Loops in the $Fe_{73.5}Cu_1Nb_3Si_{13.5}B_9$ Alloy With Small Coercivity. Front. Mater. 8:765427. doi: 10.3389/fmats.2021.765427

INTRODUCTION

Hysteresis loops are important for studying the properties of magnetic materials and often take a variety of different forms, which strongly depend on the chemical composition, the size of the magnetic materials, temperature, etc. Two important parameters to characterize the hysteresis loop are the remanence M_r and the coercive field H_c, respectively. Normally, the remanence and coercive field retain positive and negative values for the descending branch of the hysteresis loop. The positive remanence refers to the magnetization of the sample after a large magnetic field is applied. The coercivity is the reverse magnetic field to make the remanence value zero. Unlike common hysteresis loop with a counter clockwise cycle, the inverted hysteresis loop with negative remanence has a clockwise cycle and has been observed in many magnetic systems (Takanashi et al., 1993; Aharoni, 1994; Oshea and Alsharif, 1994; Ohkoshi et al., 2001; Wu et al., 2001; Kim et al., 2006; Demirtas et al., 2007; Van Tho et al., 2008; Ziese et al., 2010; Demirci et al., 2020; Ghising et al., 2020; Soldatov et al., 2020; Kumar et al., 2021) over the past decades.

In a multilayer films material, the inverted hysteresis loops were observed in Co/Pt/Gd/Pt multilayers by Takanashi et al., 1993, who considered that the origin of the inverted hysteresis loop is the interfacial exchange coupling. The phenomenon was also observed in Co/Mn/Co multilayers (Wu et al., 2001) and $La_{0.7}Sr_{0.3}MnO_3/SrRuO_3$ superlattices with ultrathin individual layers (Ziese et al., 2010; Song et al., 2013). In addition, Esho reported the inverted hysteresis loops with negative remanence in a sputtered Gd-Co alloy (Esho, 1976), and several models that are based on structural

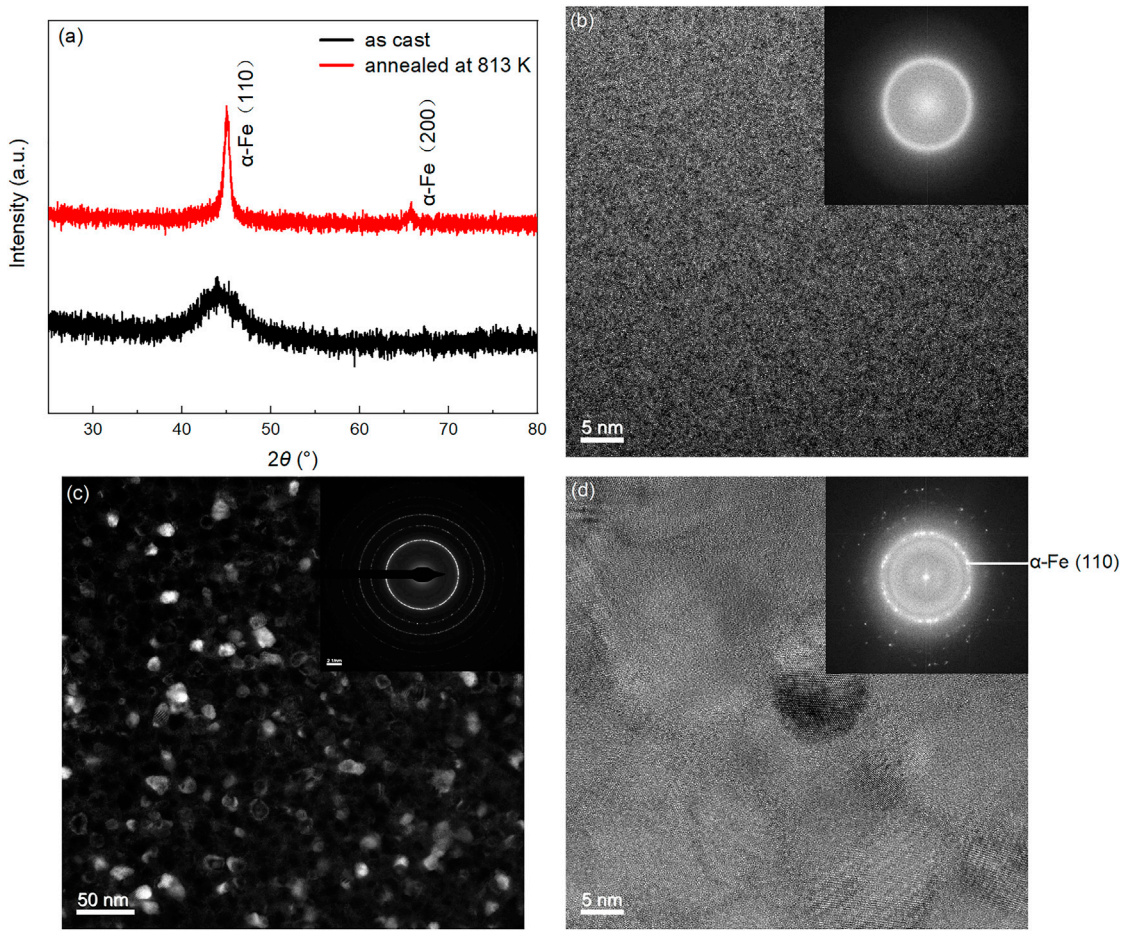

FIGURE 1 | (A) XRD patterns of the $Fe_{73.5}Cu_1Nb_3Si_{13.5}B_9$ ribbons in the as-cast state and after annealing at 813 K for 30 min in vacuum. **(B)** TEM micrograph of amorphous $Fe_{73.5}Cu_1Nb_3Si_{13.5}B_9$ ribbons. **Inset:** the associated fast Fourier transform (FFT) pattern. **(C)**–**(D)** TEM micrographs of the $Fe_{73.5}Cu_1Nb_3Si_{13.5}B_9$ ribbons annealed at 813 K for 30 min in vacuum at different magnifications. The selected area electron diffraction pattern and the associated fast Fourier transform (FFT) pattern are shown in the inset of **(C)** and **(D)**, respectively.

inhomogeneity effects have been proposed (Lutes et al., 1977; Togami, 1978). However, the anomalous hysteresis loop has also been reported on simple homogeneous systems, like pyrochlore compound $Nd_2Hf_2O_7$ and nanoparticles EuS NPs (Gu et al., 2014; Opherden et al., 2018), and it has been attributed to the competition of two anisotropies (Takanashi et al., 1993; Geshev et al., 1998; Valvidares et al., 2002; Yoon Jae and Lim, 2011). Despite the number of previous studies, the physical origin of the inverted hysteresis loop remains controversial.

Iron-based amorphous/nanocrystalline alloys have attracted considerable interests for many years since they exhibit superior magnetic softness (Fish, 1990). Among them, the nanocrystalline $Fe_{73.5}Cu_1Nb_3Si_{13.5}B_9$ alloy with a inhomogeneous structure, known as Finemet, is a frequently studied alloy owing to its high saturation magnetization M_s and low coercivity H_c (Hofmann et al., 1992; Polak et al., 1994; Gorria et al., 1996; Hofmann and Kronmüller, 1996; Barquín et al., 1998). The magnetic softness of the nanocrystalline $Fe_{73.5}Cu_1Nb_3Si_{13.5}B_9$ alloy mainly arises from the dispersion of ultrafine α-Fe(Si) grains in an amorphous matrix which reduces the effective magnetic anisotropy (Alleg et al., 2013).

In this study, we present the observation of completely inverted hysteresis loop with negative remanence in amorphous and nanocrystalline $Fe_{73.5}Cu_1Nb_3Si_{13.5}B_9$ alloys at room temperature. By comparing with the results of magnetization curve of standard Pd sample under the same conditions, we find that the net coercivities of the nanocrystalline $Fe_{73.5}Cu_1Nb_3Si_{13.5}B_9$ alloy and standard Pd sample are almost equal for the different scanning field ranges. In contrast to previous studies, we confirm the presence of the inverse hysteresis loops in $Fe_{73.5}Cu_1Nb_3Si_{13.5}B_9$ alloys is due to the remanence of superconducting magnet rather than the structural inhomogeneity effects. This may clarify the controversy about the physical origin of the inverse hysteresis loops observed in magnetic materials with small coercivity.

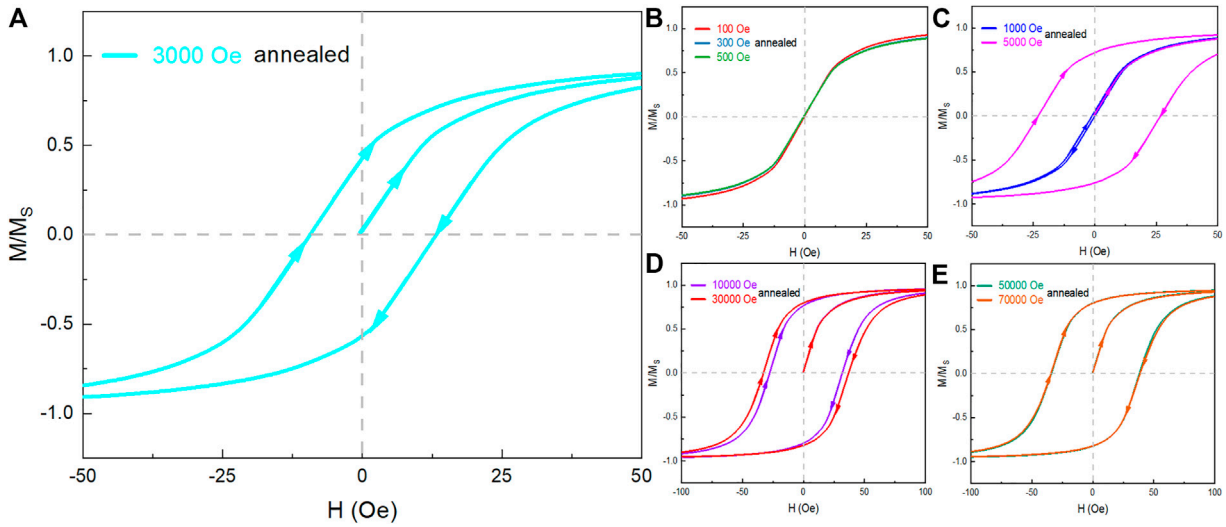

FIGURE 2 | A series of normalized *M*(*H*) loops enlarged near the origin for different scanning field ranges of nanocrystalline $Fe_{73.5}Cu_1Nb_3Si_{13.5}B_9$ sample at 300 K. The arrows stuck to the curve represent the direction of the field sweep. **(A)** Normalized *M*(*H*) loops for H_{FR} = 3000 Oe of nanocrystalline $Fe_{73.5}Cu_1Nb_3Si_{13.5}B_9$ sample. The phenomenon of inverted hysteresis loop can be observed clearly. **(B–E)** Hysteresis loops measured under different scan field ranges. At low scan fields, inverted hysteresis loop is absent as shown in **(B)**, while for higher scan fields in **(C–E)**, the loop is inverted.

EXPERIMENTAL METHODS

Amorphous ribbons of the $Fe_{73.5}Cu_1Nb_3Si_{13.5}B_9$ alloy were prepared by the spinning wheel technique on a single copper roller. Nanocrystalline alloys were obtained by means of thermal treatments of amorphous compounds of $Fe_{73.5}Cu_1Nb_3Si_{13.5}B_9$ at 813 K for 30 min in vacuum (Fujii et al., 2008), which is higher than crystallization temperature. The details were reported elsewhere (Ayers et al., 1998). The identification of amorphous and crystalline phases was measured by an X-ray (Cu *Kα*) diffraction technique at room temperature. The microstructure observation and selected area electron diffraction (ED) of the as-quenched and annealed alloys were studied using the FEI Talos F200X transmission electron microscope (TEM). A vibrating sample magnetometer (VSM) with Magnetic Property Measurement System 3 (MPMS 3 Quantum Design) was employed to measure magnetization (M) versus applied magnetic field (H) using the conventional sequence for different scan field ranges from ± 0.1 to ± 70 KOe. All measurements were carried out at 300 K, and the applied H was in the plane of the ribbons. The specimen and magnet were demagnetized in an oscillation mode at 350 K before each measurement.

RESULTS AND DISCUSSIONS

The phase of $Fe_{73.5}Cu_1Nb_3Si_{13.5}B_9$ ribbons was identified by X-ray diffraction using a diffractometer with Cu-K*α* radiation in the 2*θ* angular range of 25–80° at a scanning rate of 0.2°/s, as shown in **Figure 1A**. The diffractogram of the as-quenched sample shows a halo pattern typical for amorphous alloys. As a comparison, the X-ray diffraction pattern of the annealed sample shows the presence of a crystalline *α*-Fe solid-solution phase and an amorphous rest phase, and no other phases, except *α*-Fe(Si), were recognized from the XRD profiles, which is consistent with previous related reports (Zhang et al., 1998; Gorria et al., 2001; Majumdar and Akhtar, 2005).

In order to further characterize the morphology and microstructure of the two ribbons, transmission electron microscope tests were carried out, and the results are shown in **Figure 1B,D**. transmission electron microscope observation of the as-quenched $Fe_{73.5}Cu_1Nb_3Si_{13.5}B_9$ ribbon confirmed that the microstructure of the sample is very uniform. The high-resolution TEM (HRTEM) image (**Figure 1B**) shows a homogeneous material with no crystal lattice. Also, there is no trace of crystalline reflections in the associated fast Fourier transform (FFT) pattern. These factors indicated that the as-quenched ribbon is fully amorphous.

Figures 1C,D show the TEM microstructure images of the annealed $Fe_{73.5}Cu_1Nb_3Si_{13.5}B_9$ sample at different magnifications. The dark field image (**Figure 1C**) demonstrates that there are a lot of nanoparticles with a size around 20 nm in the annealed samples. The selected electron diffraction pattern exhibited diffraction rings for the (1 1 0) and (2 0 0) of *α*-Fe phase, as proved in the inset of **Figure 1C**. The HRTEM image of annealed ribbons demonstrated nanoparticles with a size around 20 nm embedded in an amorphous matrix, as shown in **Figure 1D**. The FFT pattern associated with **Figure 1D** reveals polycrystalline diffraction ring and a diffuse amorphous ring. The microstructures identified by TEM were a good agreement with XRD analysis results.

Magnetic hysteresis measurements using the following procedure for different scan field ranges H_{FR} from ± 0.1 to ± 70 KOe were carried out at 300 K. For each H_{FR}, the data were obtained in the conventional sequence: 0 $\rightarrow +H_{FR} \rightarrow -H_{FR}$ (descending branch) $\rightarrow +H_{FR}$ (ascending branch). In addition, the magnet was demagnetized in oscillation mode from 7 T at 350 K to eliminate remanence in the sample and magnet before each measurement. **Figure 2** shows a series of normalized magnetization loops of the annealed

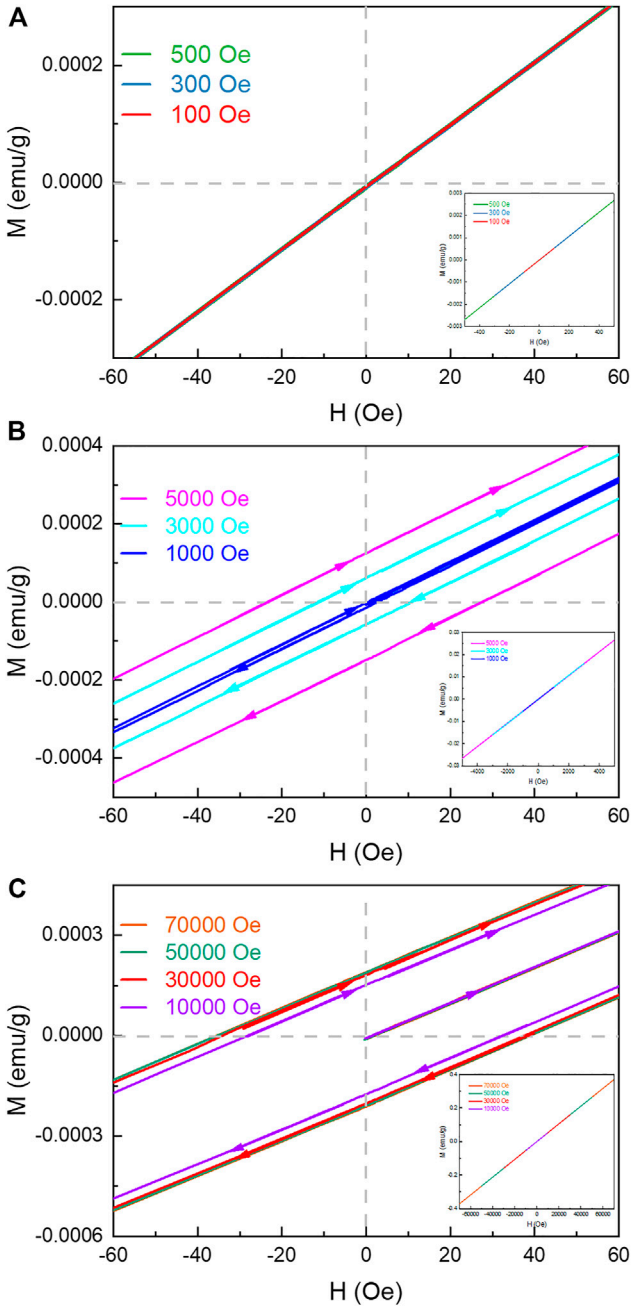

FIGURE 3 | *M*(*H*) loops enlarged near the origin for different scanning field ranges of standard Pd sample at 300 K. The arrows stuck to the curve denote the direction of the field sweep. The inset shows the full loop measured in corresponding field ranges. **(A)** At low scan fields, inverted hysteresis loop is absent for standard Pd sample. **(B,C)** *M*(*H*) loops for higher scan fields, the loop is inverted.

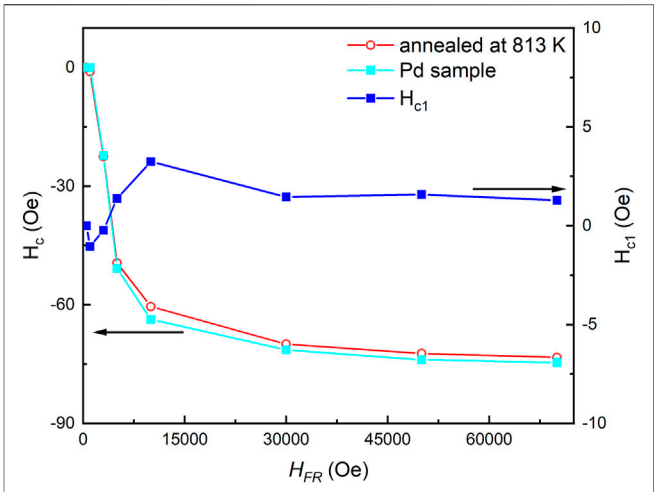

FIGURE 4 | The net coercivity H_c and H_{c1} as a function of scan field ranges H_{FR} used in hysteresis loop measurements.

$Fe_{73.5}Cu_1Nb_3Si_{13.5}B_9$ sample, which are enlarged near the central portion for a clearer understanding. The full loop measured in corresponding field ranges is shown in **Supplementary Figure S1**. In **Figure 2A**, we observed clearly the phenomenon of inverted hysteresis loop with obvious negative remanence for H_{FR} = 3000 Oe. The arrows stuck to the curve indicate the switching direction of the magnetic field. The inverted hysteresis loop with negative remanence presents a clockwise loop, which is an obvious contrast to the normal hysteresis loop with positive remanence and anticlockwise cycle. The coercivities are 12.86 Oe and −9.67 Oe for descending (H_C^{des}) and ascending (H_C^{asc}) branches, respectively. The net coercivity, defined as $H_c = H_C^{asc} - H_C^{des}$, is −22.53 Oe.

However, the magnetization curve has no hysteresis behavior and almost overlaps for different H_{FR} at low scan fields ($\leq$ 500 Oe). Meanwhile, the inversion phenomenon of hysteresis loop was absent, as can be seen from **Figure 2B**. Furthermore, the magnetization curves at other higher scan field ranges ($\geq$ 1,000 Oe) are displayed in **Figure 2C,E**. The behavior of inverted hysteresis loop begins to be observed and the corresponding coercivity values, including H_C^{des} and H_C^{asc}, are very small when the scan field range is 1,000 Oe, as shown in **Figure 2C**. With the increase of the scan field range, the phenomenon of inverted hysteresis loop becomes clearer and the coercivity increases gradually. When the scan field is above 50 KOe, the magnetization curves almost overlap and the coercivity is nearly constant ($\approx$ 72 Oe). The results of hysteresis loops for the Fe-based amorphous samples also showed similar results with that of the nanocrystalline samples (see **Supplementary Figure S2**). This indicated that the origin of the inverted hysteresis loop may not arise from the structural inhomogeneities in amorphous alloys, as proposed in previous reports (Esho, 1976; Tsujimoto and Sakurai, 1983; Oshea and Alsharif, 1994; Yan and Xu, 1996; Gu et al., 2014).

Since standard Pd sample is a paramagnetic material, the magnetization curve should be a straight line that passes through the origin and has no hysteresis. In order to further investigate the underlying origin for the inverted hysteresis loop in our specimens, the hysteresis loops of standard Pd sample were also measured following the same procedure as that of Finemet alloys at 300 K. **Figure 3** shows the *M*(*H*) loops enlarged near the origin for different scanning field ranges of standard Pd sample, and the full loops measured in corresponding field ranges is in the inset. We can see clearly that the inverted hysteresis loop is absent at low scan fields ($\leq$ 500 Oe), as

shown in **Figure 3A**. While for higher scan field ranges (≥ 1,000 Oe), the loops are inverted (see **Figures 3B,C**). When the H_{FR} = 3000 Oe, the coercivities are 11 Oe and −11.3 Oe for descending (H_C^{des}) and ascending (H_C^{asc}) branches, respectively. The net coercivity H_c is −22.3 Oe, which is very close to the results of our alloy sample.

For comparison, the net coercivity H_c of annealed sample and standard Pd sample is plotted as a function of scan field ranges H_{FR} in **Figure 4**. The net coercivity is almost zero when the applied magnetic field range is less than 1,000 Oe. However, the net coercivity increases rapidly when the magnetic field range is higher than 1,000 Oe, and it almost saturates with maximum field of 50 KOe. The H_{c1}, defined as the net coercivity difference between the annealed sample and Pd sample, is only several Oe.

Because standard Pd sample is a paramagnetic material, the deviation between the magnetization curve and the origin can reflect the remanence of the superconducting magnet, which is caused by the vortex pinning. It can be seen from **Figure 3** that when the applied magnetic field is greater than 1 KOe and then the magnetic field is removed, the superconducting magnet will have a negative remanence, and this negative remanence will increase with the increase of the applied magnetic field, even if the vibration degaussing treatment is carried out in an oscillation mode from 7T before each measurement. It indicates that the measurement results of the magnetization curve may have errors for the samples with net coercivity less than tens of Oe, which should not be ignored, when the applied magnetic field is more than 1,000 Oe. To further verify our inference, we also performed the magnetic measurement on the AlNiCo alloy with a large coercivity ~1,300 Oe using the same sequence, which is much larger than the remanence of superconducting magnet after applying a large magnetic field and then removing it. The magnetization curve of the AlNiCo alloy at 300 K represents the normal hysteresis loop with coercivity of 1,333 Oe for the H_{FR} = 7 T (see **Supplementary Figure S3** for more details). Additionally, we noted that the exchange bias $|H_{EB}|$ is almost equal to the coercivity $|H_C^{des}|$ or $|H_C^{asc}|$ for the inverted hysteresis loop at the same temperature. Therefore, the previously reported exchange bias (Maity et al., 2017; Ghising et al., 2020)) may also be caused by the remanence of superconducting magnet.

CONCLUSIONS

In conclusion, the hysteresis loop inversion was observed in the nanocrystalline $Fe_{73.5}Cu_1Nb_3Si_{13.5}B_9$ alloy ribbons and amorphous $Fe_{73.5}Cu_1Nb_3Si_{13.5}B_9$ alloy ribbons at room temperature. We prove that the phenomenon of completely inverted hysteresis loop is caused by the remanence of superconducting magnet rather than the inhomogeneity effects. We emphasize that there are slight differences in remanence for different MPMS 3 devices. Our results indicate that the results of the magnetization curve may have errors for the samples with net coercivity less than tens of Oe, which should not be ignored, when the applied magnetic field is more than 1,000 Oe using MPMS 3.

DATA AVAILABILITY STATEMENT

The original contributions presented in the study are included in the article/**Supplementary Material**; further inquiries can be directed to the corresponding author.

AUTHOR CONTRIBUTIONS

PPS performed experiments and wrote the manuscript; YTW performed the data analysis; BAS conceived the data and wrote the manuscript.

FUNDING

This research was supported by the Guangdong Major Project of Basic and Applied Basic Research of China (Grant No.2020B1515120092 and 2019B030302010), the National Key Research and Development Plan (Grant No. 2018YFA0703603), the National Natural Science Foundation of China (NSFC) (Grant No. 51822107, 11790291, and 61888102), the Strategic Priority Research Program of Chinese Academy of Sciences (Grant No. XDB30000000), and the Beijing Municipal Science & Technology Commission (No. Z191100007219006).

SUPPLEMENTARY MATERIAL

The Supplementary Material for this article can be found online at: https://www.frontiersin.org/articles/10.3389/fmats.2021.765427/full#supplementary-material.

REFERENCES

Aharoni, A. (1994). Exchange Anisotropy in Films, and the Problem of Inverted Hysteresis Loops. *J. Appl. Phys.* 76, 6977–6979. doi:10.1063/1.358061

Alleg, S., Kartout, S., Ibrir, M., Azzaza, S., Fenineche, N. E., and Suñol, J. J. (2013). Magnetic, Structural and thermal Properties of the Finemet-type Powders Prepared by Mechanical Alloying. *J. Phys. Chem. Sol.* 74, 550–557. doi:10.1016/j.jpcs.2012.12.002

Ayers, J. D., Harris, V. G., Sprague, J. A., Elam, W. T., and Jones, H. N. (1998). On the Formation of Nanocrystals in the Soft Magnetic alloy $Fe_{73.5}Nb_3Cu_1Si_{13.5}B_9$. *Acta Materialia* 46, 1861–1874. doi:10.1016/s1359-6454(97)00436-9

Barquín, L. F., Sal, J. C. G., Gorria, P., Garitaonandia, J. S., and Barandiarán, J. M. (1998). Crystal Structure and Magnetic Behaviour of Nanocrystalline Fe-Nb-Cu-Si-B Alloys Studied by Means Ofin Situneutron Diffraction. *J. Phys. Condens. Matter* 10, 5027–5038. doi:10.1088/0953-8984/10/23/009

Demirci, E., Öztürk, M., Pişkin, H., and Akdoğan, N. (2020). Angle-Dependent Inverted Hysteresis Loops in an Exchange-Biased $[Co/Pt]_5$/IrMn Thin Film. *J. Supercond Nov Magn.* 33, 721–726. doi:10.1007/s10948-019-05235-0

Demirtas, S., Hossu, M. R., Arikan, M., Koymen, A. R., and Salamon, M. B. (2007). Tunable Negative and Positive Coercivity forSmCo/(Co/Gd)exchange Springs Investigated with SQUID Magnetometry. *Phys. Rev. B* 76, 214430. doi:10.1103/physrevb.76.214430

Esho, S. (1976). Anomalous Magneto-Optical Hysteresis Loops of Sputtered Gd-Co Films. *Jpn. J. Appl. Phys.* 15, 93. doi:10.7567/jjaps.15s1.93

Fish, G. E. (1990). Soft Magnetic Materials. *Proc. IEEE* 78, 947–972. doi:10.1109/5.56909

Fujii, H., Yardley, V. A., Matsuzaki, T., and Tsurekawa, S. (2008). Nanocrystallization of $Fe_{73.5}Si_{13.5}B_9Nb_3Cu_1$ Soft-Magnetic alloy from Amorphous Precursor in a Magnetic Field. *J. Mater. Sci.* 43, 3837–3847. doi:10.1007/s10853-007-2220-7

Geshev, J., Viegas, A. D. C., and Schmidt, J. E. (1998). Negative Remanent Magnetization of fine Particles with Competing Cubic and Uniaxial Anisotropies. *J. Appl. Phys.* 84, 1488–1492. doi:10.1063/1.368214

Ghising, P., Samantaray, B., and Hossain, Z. (2020). Spin Inhomogeneities at the Interface and Inverted Hysteresis Loop in La 0.7 Sr 0.3 MnO 3/SrTiO 3. *Phys. Rev. B* 101, 024408. doi:10.1103/physrevb.101.024408

Gorria, P., Garitaonandia, J. S., and Barandiarán, J. M. (1996). Structural and Magnetic Changes in FeNbCuSiB Amorphous Alloys during the Crystallization Process. *J. Phys. Condens. Matter* 8, 5925–5939. doi:10.1088/0953-8984/8/32/012

Gorria, P., Prida, V. M., Tejedor, M., Hernando, B., and Sánchez, M. L. (2001). Correlation between Structure, Magnetic Properties and MI Effect during the Nanocrystallisation Process of FINEMET Type Alloys. *Physica B: Condensed Matter* 299, 215–224. doi:10.1016/s0921-4526(01)00468-9

Gu, S., He, W., Zhang, M., Zhuang, T., Jin, Y., ElBidweihy, H., et al. (2014). Physical Justification for Negative Remanent Magnetization in Homogeneous Nanoparticles. *Scientific Rep.* 4, 6267. doi:10.1038/srep06267

Hofmann, B., and Kronmüller, H. (1996). Stress-induced Magnetic Anisotropy in Nanocrystalline FeCuNbSiB alloy. *J. Magnetism Magn. Mater.* 152, 91–98. doi:10.1016/0304-8853(95)00447-5

Hofmann, B., Reininger, T., and Kronmüller, H. (1992). Influence of the Microstructure on the Magnetization Processes in Nanocrystalline $Fe_{73.5}Cu_1Nb_3Si_{13.5}B_9$. *Phys. Stat. Sol. (A)* 134, 247–261. doi:10.1002/pssa.2211340122

Kim, D., Kim, C., Kim, C. O., Yoon, S. S., Naka, M., Tsunoda, M., et al. (2006). Negative Coercivity Characteristics in Antiferromagnetic Coupled Hard/soft Multilayers. *J. Magnetism Magn. Mater.* 304, E356. doi:10.1016/j.jmmm.2006.01.198

Kumar, R., Sarangi, S. N., Samal, D., and Hossain, Z. (2021). Positive Exchange Bias and Inverted Hysteresis Loop in Y 3 Fe 5 O 12/Gd 3 Ga 5 O 12. *Phys. Rev. B* 103, 064421. doi:10.1103/physrevb.103.064421

Lutes, O., Holmen, J., Kooyer, R., and Aadland, O. (1977). Inverted and Biased Loops in Amorphous Gd-Co Films. *IEEE Trans. Magn.* 13, 1615–1617. doi:10.1109/tmag.1977.1059654

Maity, T., Kepaptsoglou, D., Schmidt, M., Ramasse, Q., and Roy, S. (2017). Observation of Complete Inversion of the Hysteresis Loop in a Bimodal Magnetic Thin Film. *Phys. Rev. B* 95, 100401. doi:10.1103/physrevb.95.100401

Majumdar, B., and Akhtar, D. (2005). Structure and Coercivity of Nanocrystalline Fe-Si-B-Nb-Cu Alloys. *Bull. Mater. Sci.* 28, 395–399. doi:10.1007/bf02711225

Ohkoshi, S.-i., Hozumi, T., and Hashimoto, K. (2001). Design and Preparation of a Bulk Magnet Exhibiting an Inverted Hysteresis Loop. *Phys. Rev. B* 64, 132404. doi:10.1103/physrevb.64.132404

Opherden, L., Bilitewski, T., Hornung, J., Herrmannsdörfer, T., Samartzis, A., Islam, A. T. M. N., et al. (2018). Inverted Hysteresis and Negative Remanence in a Homogeneous Antiferromagnet. *Phys. Rev. B* 98, 180403. doi:10.1103/physrevb.98.180403

Oshea, M. J., and Alsharif, A. L. (1994). Inverted Hysteresis in Magnetic Systems With Interface Exchange. *J. Appl. Phys.* 75, 6673. doi:10.1063/1.356891

Polak, C., Knobel, M., Grossinger, R., and Turtelli, R. S. (1994). The Development of Nanocrystalline $Fe_{73.5}Cu_1Nb_3Si_{13.5}B_9$: Magnetism and Structural Disorder. *J. Magnetism Magn. Mater.* 134, 6977. doi:10.1016/0304-8853(94)90065-5

Soldatov, I., Andrei, P., and Schaefer, R. (2020). Inverted Hysteresis, Magnetic Domains, and Hysterons. *Ieee Magnetics Lett.* 11, 2405805. doi:10.1109/lmag.2020.3035136

Song, C., Cui, B., Yu, H. Y., and Pan, F. (2013). Completely Inverted Hysteresis Loops: Inhomogeneity Effects or Experimental Artifacts. *J. Appl. Phys.* 114, 183906. doi:10.1063/1.4830011

Takanashi, K., Kurokawa, H., and Fujimori, H. (1993). A Novel Hysteresis Loop and Indirect Exchange Coupling in Co/Pt/Gd/Pt Multilayer Films. *Appl. Phys. Lett.* 63, 1585–1587. doi:10.1063/1.110756

Togami, Y. (1978). Stability of Small Bits Written in Amorphous GdCo Thin Films. *Appl. Phys. Lett.* 32, 673–675. doi:10.1063/1.89851

Tsujimoto, H., and Sakurai, Y. (1983). Temperature Dependence of Anomalous Loop in Double-Layered Amorphous GdCo Film. *Jpn. J. Appl. Phys.* 22, 1845–1850. doi:10.1143/jjap.22.1845

Valvidares, S. M., Martı´n, J. I., Álvarez-Prado, L. M., Pain, D., Acher, O., Suran, G., et al. (2002). Inverted Hysteresis Loops in Annealed Co-Nb-zr and Co-Fe-Mo-Si-B Amorphous Thin Films. *J. Magnetism Magn. Mater.* 242-245, 169–172. doi:10.1016/s0304-8853(01)01195-7

Van Tho, L., Kim, C. G., and Kim, C. O. (2008). Investigation of Negative Coercivity in One Layer Formation of Soft and Hard Magnetic Materials. *J. Appl. Phys.* 103 (3), 07b906. doi:10.1063/1.2830966

Wu, Y. Z., Dong, G. S., and Jin, X. F. (2001). Negative Magnetic Remanence in Co/Mn/Co Grown on GaAs(001). *Phys. Rev. B* 64 (5), 214406. doi:10.1103/physrevb.64.214406

Yan, X., and Xu, Y. (1996). Negative Remanence in Magnetic Nanostructures. *J. Appl. Phys.* 79, 6013. doi:10.1063/1.362137

Yoon Jae, N., and Lim, S. H. (2011). Negative Remanent Magnetization in a Single Domain Particle with Two Uniaxial Anisotropies. *Appl. Phys. Lett.* 99, 092503. doi:10.1063/1.3633107

Zhang, X. Y., Zhang, F. X., Zhang, J. W., Yu, W., Zhang, M., Zhao, J. H., et al. (1998). Influence of Pressures on the Crystallization Process of an Amorphous $Fe_{73.5}Cu_1Nb_3Si_{13.5}B_9$ alloy. *J. Appl. Phys.* 84, 1918–1923. doi:10.1063/1.368319

Ziese, M., Vrejoiu, I., and Hesse, D. (2010). Inverted Hysteresis and Giant Exchange Bias in La0.7Sr0.3MnO3/SrRuO3 Superlattices. *Appl. Phys. Lett.* 97, 052504. doi:10.1063/1.3470101

Conflict of Interest: The authors declare that the research was conducted in the absence of any commercial or financial relationships that could be construed as a potential conflict of interest.

Publisher's Note: All claims expressed in this article are solely those of the authors and do not necessarily represent those of their affiliated organizations, or those of the publisher, the editors, and the reviewers. Any product that may be evaluated in this article, or claim that may be made by its manufacturer, is not guaranteed or endorsed by the publisher.

Copyright © 2021 Shen, Wang and Sun. This is an open-access article distributed under the terms of the Creative Commons Attribution License (CC BY). The use, distribution or reproduction in other forums is permitted, provided the original author(s) and the copyright owner(s) are credited and that the original publication in this journal is cited, in accordance with accepted academic practice. No use, distribution or reproduction is permitted which does not comply with these terms.